Electrogenerated Chemiluminescence Behavior of Graphite-like Carbon Nitride and Its Application in Selective Sensing Cu^{2+}

Changming Cheng,[†] Ying Huang,[†] Xianqing Tian,[‡] Baozhan Zheng,[‡] Yi Li,[†] Hongyan Yuan,[†] Dan Xiao,*[,†,‡] Shunping Xie,[§] and Martin M. F. Choi*[,§]

[†]College of Chemical Engineering, Sichuan University, Chengdu 610065, PR China
[‡]College of Chemistry, Sichuan University, Chengdu 610064, PR China
[§]Department of Chemistry, Hong Kong Baptist University, 224 Waterloo Road, Kowloon Tong, Hong Kong SAR, PR China

S *Supporting Information*
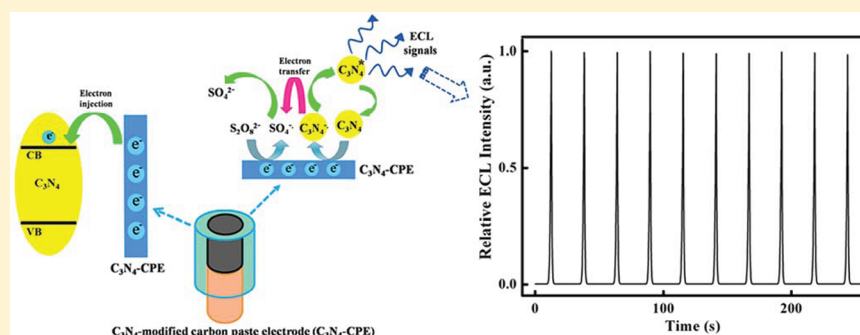
ABSTRACT: This paper reports for the first time the electrogenerated chemiluminescence (ECL) behavior of graphite-like carbon nitride (g-C$_3$N$_4$) with K$_2$S$_2$O$_8$ as the coreactant. The possible ECL reaction mechanisms are proposed. The spectral features of the ECL emission and photoluminescence (PL) of g-C$_3$N$_4$ are compared, and their resemblance demonstrates that the excited states of g-C$_3$N$_4$ from both ECL and photoexcitation are the same. The effects of K$_2$S$_2$O$_8$ concentration, pH, g-C$_3$N$_4$/ carbon powder ratio, and scan rate on the ECL intensity have been studied in detail. Furthermore, it is observed that the ECL intensity is efficiently quenched by trace amounts of Cu^{2+}. g-C$_3$N$_4$ is thus employed to fabricate an ECL sensor which shows high selectivity to Cu^{2+} determination. The limit of detection is determined as 0.9 nM. It is anticipated that g-C$_3$N$_4$ could be a new class of promising material for fabricating ECL sensors.

In the present work, we report for the first time the electrogenerated chemiluminescence (ECL) of graphite-like carbon nitride (g-C$_3$N$_4$), which has recently attracted considerable attention attributing to its special structure and properties. Since g-C$_3$N$_4$ is a chemically and thermally stable semiconductor with a band gap of ca. 2.7 eV,[1] it has been explored for various applications, especially in the fields of catalysis and degradation.[1−9] For instance, the generation of hydrogen from water could be realized by just the use of the inexpensive g-C$_3$N$_4$ as stable photocatalyst without any noble metals.[1] Furthermore, the semiconductor g-C$_3$N$_4$ exhibits good performance in hydrocarbon oxidation,[2−4] carbon dioxide/ oxygen reduction,[5] organic dye degradation,[6,7] phenol hydrogenation,[8] and Friedel−Crafts reaction.[9] It has also been reported that g-C$_3$N$_4$ exhibits photovoltaic/photocurrent effect, which is complement to other photoactive materials in the solar energy converting system.[10,11] Additionally, an optical sensing system based on mesoporous g-C$_3$N$_4$ has been applied for detection of trace metal ions in aqueous solutions, where g-C$_3$N$_4$ as Lewis base shows high adsorption capacity for metal ions via chelation, initiating the promise for future biological and environmental monitoring.[12]

The ultraviolet−visible (UV−vis) absorption and photoluminescence (PL) spectra of g-C$_3$N$_4$ have been well-documented in previous reports.[7,12,13] The absorption spectrum provides information about the band gap of this semiconductor, whereas the emission spectrum in the blue wavelength region implies that g-C$_3$N$_4$ could be utilized as an emitting material in light-emitting diodes and display devices. Recently, diverse semiconductors have been widely studied in the ECL field due to their unique ECL properties and potential applications in chemical sensors and biosensors.[14−27] ECL exhibits attractive features over the PL technique because of its simpler design, lower cost, lower background emission, better controllability, and higher sensitivity.[15,28−30] g-C$_3$N$_4$ possesses good chemical and thermal stability at ambient conditions,[4,6,11] attributing to the strong covalent bonds between the carbon and nitrogen atoms. It is inexpensive and nontoxic and can be prepared by a simple thermal pyrolysis method. However, to the best of our knowledge, the ECL of g-C$_3$N$_4$ has never been

reported. As such, it is our goal to investigate the ECL behavior of g-C$_3$N$_4$ and expand its potential applications in the analytical chemistry field.

In this work, the ECL measurements are conducted in 0.10 M potassium sulfate (K$_2$SO$_4$) aqueous solution containing potassium peroxydisulfate (K$_2$S$_2$O$_8$) as the coreactant by cyclic voltammetry (CV). The possible ECL reaction mechanisms are proposed. The electro-reduced g-C$_3$N$_4$ can readily react with a coreactant to produce an excited state which subsequently decays back to its ground state, emitting strong luminescence. The ECL displays a maximum emission peak at ca. 470 nm, which matches well with the PL spectrum of g-C$_3$N$_4$, suggesting that the same excited states are formed in both the electro-excitation and photoexcitation processes. Factors affecting the ECL response were studied carefully and the ECL working conditions were optimized. In addition, g-C$_3$N$_4$ could be used to fabricate an ECL sensor which shows high selectivity for detection of trace Cu^{2+} in nanomolar concentration. Cu^{2+} is a common pollutant in the environment. It is also a trace and essential element in biological systems.[26,27,31] The application of this type of ECL sensor in real sample analysis is examined. The findings would open new avenues to construct ECL analytical systems based on semiconductor g-C$_3$N$_4$ material as it is stable and cost-effective.

■ EXPERIMENTAL SECTION

Chemicals. Melamine (2,4,6-triamino-1,3,5-trazine, 95%) was purchased from Kelong Chemical Co., Ltd. (Chengdu, China). Carbon powder (SP grade), potassium peroxydisulfate (AR grade), and potassium sulfate (AR grade) were obtained from Shanghai Chemical Reagent Co., Ltd. (Shanghai, China). All other reagents of analytical grade were used as received without further purification. Double distilled water was used throughout.

Synthesis of g-C$_3$N$_4$. g-C$_3$N$_4$ was prepared as described previously with some slight modifications.[6,32] In brief, 5.0 g of white melamine powder was placed into a semiclosed ceramic crucible and heated at 823 K for 4 h in a muffle furnace under open air condition. Then, the sample was cooled to room temperature to obtain the yellow g-C$_3$N$_4$ product. It was ground to powder for further use.

Characterization. Powder X-ray diffraction (XRD) measurements were performed on a Tongda TD-3500 X-ray diffractometer (Dandong, Liaoning, China) with Cu Kα radiation in a symmetric reflection setup. The PL and ECL emission spectra were recorded on a Hitachi F-7000 fluorescence spectrophotometer (Tokyo, Japan). The ECL behavior of g-C$_3$N$_4$ was investigated on a g-C$_3$N$_4$-modified carbon paste electrode. Herein, the carbon paste electrode was used as the working electrode owing to its broad potential window, low background current, chemical inertness, and ease of fabrication. Known quantities of carbon powder and g-C$_3$N$_4$ were thoroughly mixed with paraffin oil to obtain a homogeneous paste. Then, the paste was packed into a glass tube and connected to a copper wire for electrical contact. The electrode surface (2.0 mm in diameter) was polished with a piece of smooth paper before electrochemical measurements. For comparison, a pure carbon paste electrode without g-C$_3$N$_4$ was also prepared.

The CV and ECL measurements were conducted at 298 K in a classical three-electrode configuration consisting of a g-C$_3$N$_4$-modified carbon paste electrode working electrode, a platinum counter electrode, and an Ag/AgCl reference electrode. The CV and ECL curves were recorded simultaneously using a MPI-E electrochemiluminescence analyzer system (Xi'an Remax Analysis Instrument Co., Ltd., Xi'an, China). The supporting electrolyte was 0.10 M K$_2$SO$_4$ with or without K$_2$S$_2$O$_8$ as the ECL coreactant. The photographic ECL image of g-C$_3$N$_4$ coated on a square indium tin oxide (ITO) glass plate was captured by a commercial digital camera in a dark environment.

■ RESULTS AND DISCUSSION

Synthesis and ECL Behavior of g-C$_3$N$_4$. In order to identify the phase structure of the as-synthesized sample, XRD measurement was conducted and is displayed in Figure S1 (Supporting Information). The XRD pattern is in good agreement with that of g-C$_3$N$_4$ in the previous report.[6] In this study, the synthesis process was simplified by a one-step thermal-induced self-condensation of melamine under atmospheric environment and was done without the protection of inert gas. Figure 1 displays the ECL curves of the g-C$_3$N$_4$-
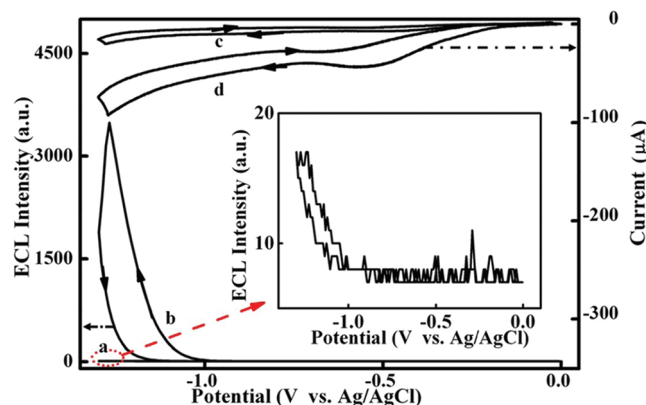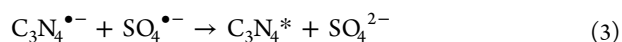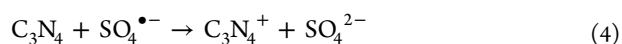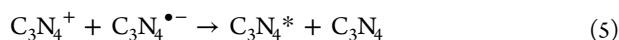

Figure 1. ECL–potential (a, b) and CV (c, d) curves of the g-C$_3$N$_4$-modified carbon paste electrode in 0.10 M K$_2$SO$_4$ without (a, c) and with (b, d) 3.0 mM K$_2$S$_2$O$_8$. The scan rate is 100 mV/s. The inset displays the enlarged view of curve a.

modified carbon paste electrode in the absence (curve a) and presence (curve b) of K$_2$S$_2$O$_8$ by cycling the potential between 0.00 and −1.30 V. An intense ECL emission is obtained on the g-C$_3$N$_4$-modified carbon paste electrode with 3.0 mM K$_2$S$_2$O$_8$. In contrast, only a very weak ECL is obtained without K$_2$S$_2$O$_8$ as shown in the inset of Figure 1. Obviously, these results confirm that the coreactant K$_2$S$_2$O$_8$ could greatly enhance the ECL intensity, inferring that S$_2$O$_8$$^{2-}$ must play a crucial role in the ECL process. Two main ECL mechanisms, i.e., ion annihilation ECL and coreactant ECL, have been proposed in the literature.[33−35] Analogous to the ECL pathways of other semiconductors and Au nanoclusters,[29,34,36] the possible electrochemical reactions of g-C$_3$N$_4$ and S$_2$O$_8$$^{2-}$ on the carbon paste electrode are as follows:

$$C_3N_4 + e^- \rightarrow C_3N_4^{\bullet-} \tag{1}$$

$$S_2O_8^{2-} + e^- \rightarrow SO_4^{2-} + SO_4^{\bullet-} \tag{2}$$

$$C_3N_4^{\bullet-} + SO_4^{\bullet-} \rightarrow C_3N_4^* + SO_4^{2-} \tag{3}$$

and/or

$$C_3N_4 + SO_4^{\bullet-} \rightarrow C_3N_4^+ + SO_4^{2-} \tag{4}$$

$$C_3N_4^+ + C_3N_4^{\bullet-} \rightarrow C_3N_4^* + C_3N_4 \qquad (5)$$

finally,

$$C_3N_4^* \rightarrow C_3N_4 + h\nu \qquad (6)$$

It has been reported that electrochemically reduced semiconductors could react with coreactants to produce ECL.[18,23,36,37] Herein, an electron from the working electrode is injected to the conduction band of the semiconductor g-C_3N_4 to produce the negatively charged semiconductor g-C_3N_4 (i.e., g-$C_3N_4^{\bullet-}$) (eq 1) during the cathodic potential scan as the potential is negative enough. Furthermore, there is evidence of electron injection to the conduction band of g-C_3N_4. For instance, electron from poly(3-hexylthiophene) can be injected into the conduction band of g-C_3N_4 in the photocatalytic hydrogen production process.[32] The electronic band gaps of g-C_3N_4 have been previously explored, and the edge positions of the conduction band and the valence band are −0.83 and 1.83 V (vs NHE), respectively.[10] As such, it is energetically possible for electron transfer from the carbon paste electrode to the conduction band of g-C_3N_4 if the applied potential on the working electrode is more negative than that of the conduction band of g-C_3N_4. Figure 1 depicts the CV curves of the g-C_3N_4-modified carbon paste electrodes in 0.10 M K_2SO_4 aqueous solution in the absence (curve c) and presence of $K_2S_2O_8$ (curve d). The reduction current increases sharply when the scan potential is more negative than ca. −1.00 V (vs Ag/AgCl) attributing to the electro-reduction of g-C_3N_4. For comparison, similar CV scans were conducted on the pure carbon paste electrode and are shown in Figure S2 (Supporting Information). The cathodic current is much smaller than that of the g-C_3N_4-modified carbon paste electrode. These data confirm the electron injection process shown in eq 1.

Figure 1 displays that a broad cathodic wave with a small shoulder peak at ca. −0.55 V (vs Ag/AgCl) is found for the g-C_3N_4-modified carbon paste electrode with $K_2S_2O_8$ (curve d). In contrast, a small cathodic wave without a shoulder peak is found when no $K_2S_2O_8$ is used (curve c). It is possible that $S_2O_8^{2-}$ is electro-reduced to $SO_4^{\bullet-}$ and SO_4^{2-} (eq 2).[29,38,39] Similar CV scans were conducted on the pure carbon paste electrode with $K_2S_2O_8$ (curve b in Figure S2, Supporting Information). A broad reduction peak of $S_2O_8^{2-}$ at ca. −0.85 V (vs. Ag/AgCl) is observed which is more negative than that of the g-C_3N_4-modified carbon paste electrode (−0.55 V), indicating that $S_2O_8^{2-}$ could be more favorably electro-reduced on the g-C_3N_4 semiconductor. The strong oxidant species ($SO_4^{\bullet-}$) produced from electro-reduction during the cathodic scan (eq 2)[40,41] would subsequently react with the reduced form of g-C_3N_4 to produce the excited state g-C_3N_4 (g-$C_3N_4^*$) via electron transfer from g-$C_3N_4^{\bullet-}$ to $SO_4^{\bullet-}$ (eq 3). Another possible pathway for the generation of g-$C_3N_4^*$ can be described by eqs 4 and 5. Since $SO_4^{\bullet-}$ is a very powerful oxidant, it may oxidize g-C_3N_4 to g-$C_3N_4^+$ (eq 4) which is analogous to the formation of aromatic hydrocarbons radical cation upon oxidation by $SO_4^{\bullet-}$.[42] Subsequently, the annihilation of g-$C_3N_4^+$ and g-$C_3N_4^{\bullet-}$ ions produces the ground state and excited state g-C_3N_4 (eq 5). Finally, an intense blue emission is obtained when g-$C_3N_4^*$ decays back to the ground state g-C_3N_4 (eq 6). The onset potential for ECL is at ca. −1.00 V (vs Ag/AgCl), concurring with the electrochemical reduction of g-C_3N_4.

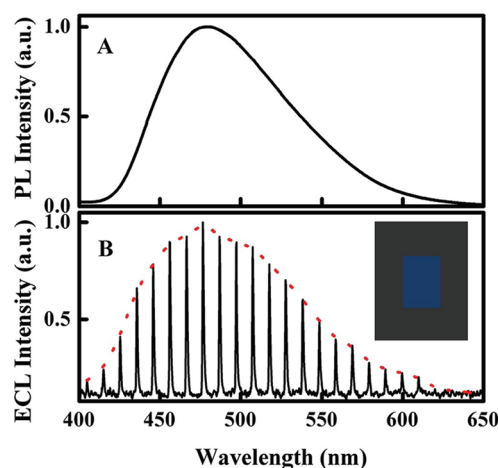Figure 2A displays the PL spectrum of g-C_3N_4 solid powder at an excitation wavelength of 365 nm. A broad emission band

Figure 2. (A) PL spectrum of g-C_3N_4 solid powder when excited at 365 nm and (B) ECL spectrum of the g-C_3N_4-modified electrode in 0.10 M K_2SO_4 containing 3.0 mM $K_2S_2O_8$ by cycling the potential between 0.00 and −1.30 V (vs Ag/AgCl) with 1 mV step potential. The red curve is drawn across the ECL peaks to illustrate the ECL spectrum. The inset displays the photographic ECL image of g-C_3N_4 on an ITO glass.

at ca. 400−650 nm and an emission peak of ca. 470 nm are observed. The PL emission is derived from the electron−hole recombination process of g-C_3N_4 after the charge separation of the electron (in the conduction band) and the hole (in the valence band) upon photoexcitation.[7,32] Figure 2B depicts the ECL spectrum of g-C_3N_4-modified electrode in 0.10 M K_2SO_4 and 3.0 mM $K_2S_2O_8$, recorded on a fluorescence spectrophotometer, with potentials cycling between 0.00 and −1.30 V at a scan rate of 100 mV/s and step potential of 1 mV. A red curve is drawn across all the peaks to better illustrate the ECL spectrum which matches closely with the PL band of g-C_3N_4. The energy of the ECL peak (ca. 470 nm, 2.6 eV) basically agrees with the optical band gap energy (2.7 eV), indicating that ECL emission is the band gap luminescence,[7] which is consistent with other semiconductors.[21] The ECL spectrum is slightly broader than the PL spectrum as a consequence of the differences in spectral measurements. The PL spectrum was recorded using g-C_3N_4 solid powder under photoexcitation whereas the ECL spectrum was acquired from a solution containing a coreactant. This is similar to our previous findings.[43] The spectral feature of ECL indicates that the excited-state g-C_3N_4 (g-$C_3N_4^*$) generated from the electrochemical reactions is similar to that from photoexcitation. The blue ECL emission from g-C_3N_4 is strong enough to be observed with naked eyes as shown in the inset of Figure 2B. The ECL intensities of the g-C_3N_4-modified carbon paste electrode in 0.10 M K_2SO_4 solution containing 3.0 mM $K_2S_2O_8$ and the carbon paste electrode in a standard solution of 0.10 M K_2SO_4 containing 3.0 mM $K_2S_2O_8$ and 1.0 mM Ru(bpy)$_3^{2+}$ were compared. The ECL intensity of g-C_3N_4 is about 0.13 times of that of the standard solution (Figure S3, Supporting Information), demonstrating that our ECL sensor produces reasonable emission intensity.

Optimization of ECL Working Conditions. The ECL signal from the g-C_3N_4-modified carbon paste electrode is affected by several factors including $K_2S_2O_8$ concentration, solution pH, ratio of g-C_3N_4 to carbon powder (w/w), and CV scan rate. The ECL working conditions were optimized in this work. Figure 3A depicts the effect of $K_2S_2O_8$ concentration
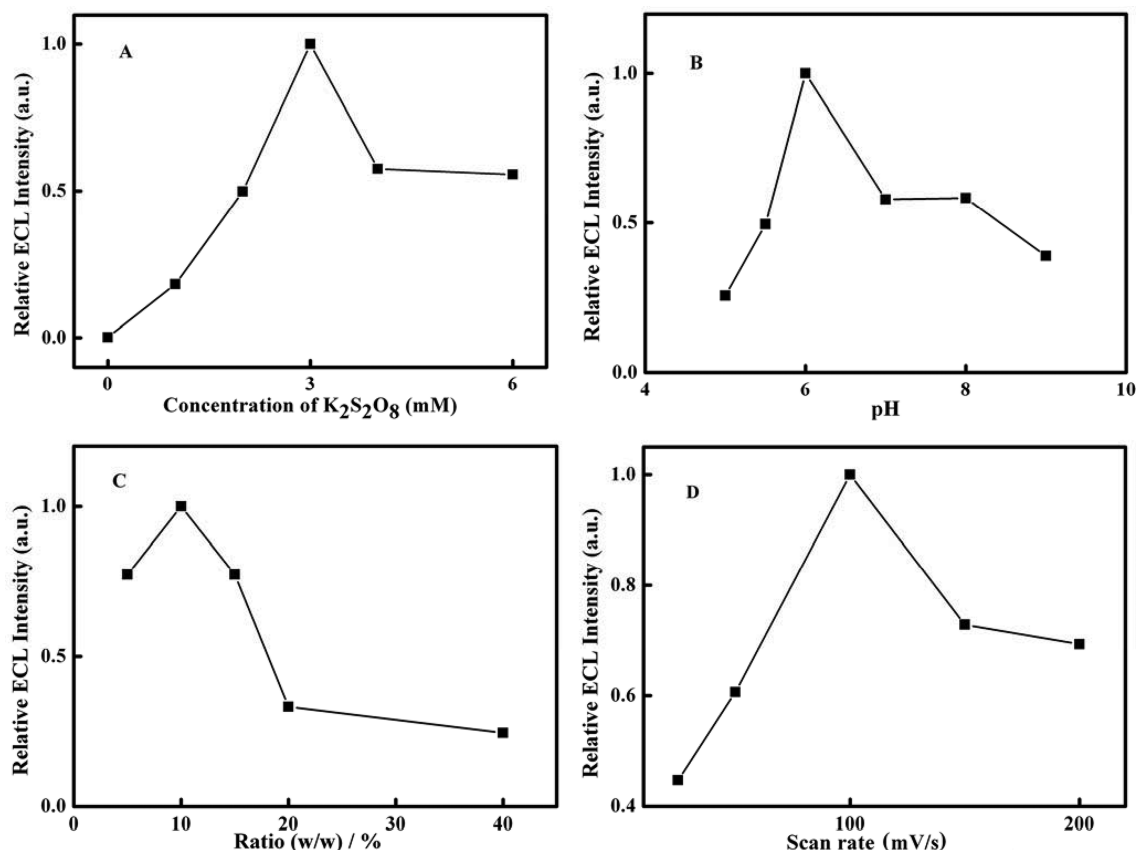
Figure 3. Effects of (A) $K_2S_2O_8$ concentration, (B) solution pH, (C) the ratio of g-C_3N_4 to carbon powder, and (D) scan rate on the ECL intensity of the g-C_3N_4-modified carbon paste electrode.

(0.0−6.0 mM) on the ECL intensity of the g-C_3N_4-modified carbon paste electrode. The ECL intensity increases significantly with the increase in $K_2S_2O_8$ concentration from 0.0 to 3.0 mM because more g-C_3N_4* is produced from oxidation of the negatively charged g-C_3N_4 by the electrogenerated $SO_4^{\bullet-}$. Further increase in $K_2S_2O_8$ concentration causes the decrease in ECL intensity as excess $S_2O_8^{2-}$ would react readily with the negatively charged g-C_3N_4 which inhibits the formation of the excited-state g-C_3N_4*. A similar phenomenon was reported in the literature.[38,41] As such, 3.0 mM was chosen as the optimal $K_2S_2O_8$ concentration and used throughout this work.

Figure 3B displays the effect of electrolyte pH (5.0−9.0) on the ECL intensity. The ECL intensity increases with the increase in pH 5.0−6.0 and then drops at high pH 6.0−9.0. At low pH, the proton could be reduced easily at the negative potential and the electro-reduction of g-C_3N_4 is inhibited. At too high pH, the strong oxidant $SO_4^{\bullet-}$ is consumed via the scavenging effect of OH^-.[38,41,44] As a result, too low or high pH causes the decrease in the ECL intensity of the g-C_3N_4-modified carbon paste electrode. Thus, pH 6.0 was chosen for this work as it would produce the strongest ECL emission.

The amount of g-C_3N_4 for fabrication of g-C_3N_4-modified carbon paste was investigated. Figure 3C depicts the ECL intensities of various g-C_3N_4-modified carbon paste electrodes with different ratios of g-C_3N_4 to carbon powder. The ECL intensity increases with the increase of g-C_3N_4 (5−10% w/w) and then decreases with further increase in g-C_3N_4, attributing to the self-absorption effect of the luminophor.[25,45] Since g-C_3N_4 exhibits strong absorption and ECL emission in the wavelength range of 300−450 nm[1,7] and 400−650 nm (Figure

2B), respectively, there is a partial overlap of these spectra; thus, self-absorption occurs easily especially when the amount of g-C_3N_4 is high. As a result, 10% w/w g-C_3N_4 was used for fabrication of the g-C_3N_4-modified carbon paste electrode.

Finally, the effect of scan rate on the ECL intensity was investigated and displayed in Figure 3D. The ECL intensity increases steadily with the increase in scan rate (25−100 mV/s) and then decreases at scan rates of 100−200 mV/s. These results are consistent with other ECL sensors.[46,47] The ECL efficiency is governed by the formation rate of the excited-state species as well as the diffusion rate of the coreactant.[46] At high scan rates, the consumption of coreactant on the electrode interface would be much faster than the diffusion of the coreactant from the bulk solution to the electrode surface, leading to a low transient concentration of coreactant near the surface of the electrode with a concomitant decrease in ECL. In summary, too high of a scan rate would decrease the ECL; thus, 100 mV/s was selected as the optimal scan rate in this work.

Application of ECL from g-C_3N_4. Operational stability is one of the major concerns for practical application of a sensor. Figure 4 displays the ECL emission of the g-C_3N_4-modified carbon paste electrode under ten cycles of continuous potential scans between 0.00 and −1.30 V (vs Ag/AgCl) in 0.10 M K_2SO_4 (pH 6.0) and 3.0 mM $K_2S_2O_8$ at 100 mV/s. Strong and stable ECL signals are observed with a relative standard deviation of 0.36%. The results signify the excellent reversibility of the ECL signal, inferring its potential as an ECL sensor.

It was reported that the ECL emission based on other semiconductors could be quenched statically by Cu^{2+}.[22,26] In this work, it is found that the ECL intensity of the g-C_3N_4-
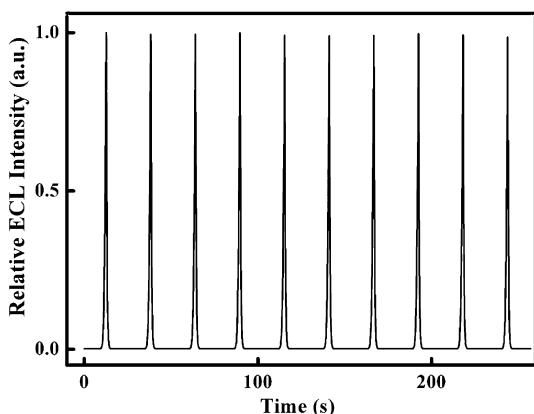
Figure 4. Stability of ECL emissions from the g-C$_3$N$_4$-modified carbon paste electrode under ten continuous cycles of CV scan.

modified carbon paste electrode is effectively quenched by trace amounts of Cu^{2+}, demonstrating its potential for Cu^{2+} determination. Figure 5 presents the effect of various
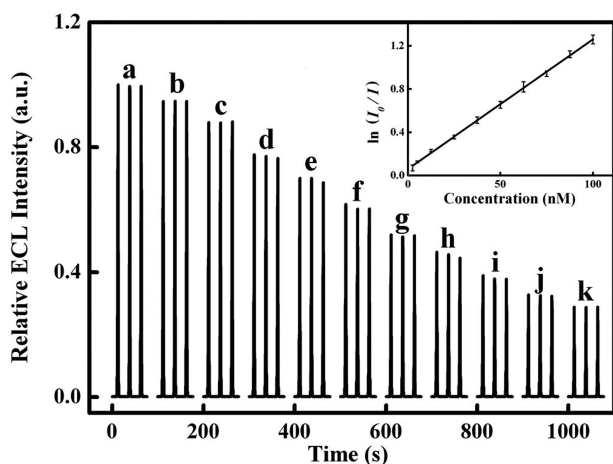

Figure 5. Effect of the concentration of Cu^{2+} (a) 0.0, (b) 2.5, (c) 5.0, (d) 12.5, (e) 25.0, (f) 37.5, (g) 50.0, (h) 62.5, (i) 75.0, (j) 87.5, and (k) 100.0 nM on the ECL intensity of the g-C$_3$N$_4$-modified carbon paste electrode. The inset displays the plot of ln(I_o/I) against the concentration of Cu^{2+}, where I_o and I are the ECL intensities in the absence and presence of Cu^{2+}, respectively.

concentrations of Cu^{2+} on the ECL intensity of the g-C$_3$N$_4$-modified carbon paste electrode. Clearly, the ECL intensity decreases with the increase in Cu^{2+} concentration. Cu^{2+} could effectively quench the ECL of the g-C$_3$N$_4$-modified carbon paste electrode in the nanomolar range. The Poisson statistics static quenching model[26,48,49] was employed to linearly relate the decrease in ECL intensity and concentration of Cu^{2+} by plotting ln(I_o/I) against the concentration of Cu^{2+} as shown in the inset of Figure 5, where I_o and I are the ECL intensities in the absence and presence of Cu^{2+}. The curve has a linear range from 2.5 to 100 nM with a detection limit of 0.9 nM (S/N = 3), which is lower than or comparable with other optical Cu^{2+} sensors based on semiconductor materials.[12,22,26] The main attribute of the proposed ECL sensor is that the fabrication process is simple and cost-effective. More importantly, it exhibits potential for detection of Cu^{2+} in the subnanomolar level.

The selectivity of the present ECL sensor was also examined using common metal ions as potential interfering agents. The g-C$_3$N$_4$-modified carbon paste electrodes were exposed to these metal ions (100 nM) in 0.10 M K$_2$SO$_4$ (pH 6.0) and 3.0 mM K$_2$S$_2$O$_8$. Figure S4 (Supporting Information) reveals that the present ECL sensor has an excellent selectivity for Cu^{2+} over the other metal ions. Co^{2+}, Zn^{2+}, K$^+$, Ca^{2+}, Mg^{2+}, Fe^{2+}, Ni^{2+}, Pb^{2+}, and Cd^{2+} ions exhibit small quenching effects on the ECL signals which are similar to that of the PL measurement.[12] The proposed ECL sensor shows excellent selectivity to Cu^{2+} detection which could be attributed to the redox potential of Cu^{2+}/Cu (0.159 V vs NHE) lying between the conduction (−0.83 V) and the valence bands (1.83 V) of g-C$_3$N$_4$ that allows efficient electron transfer from the negatively charged g-C$_3$N$_4$ to Cu^{2+}, resulting in quenching of ECL.[10] In addition, since the redox potential of Cu^{2+} is more positive than the other metal ions, the electron transfer between Cu^{2+} and g-C$_3$N$_4$ is more favorable than between other metal ions (i.e., Co^{2+}, Zn^{2+}, and Fe^{2+}).

To further demonstrate the analytical reliability and real application of the developed ECL sensor, it was applied to determine the concentration of Cu^{2+} in a wastewater sample from a local factory. Wastewater sample (5.0 μL) was directly injected into the 5.0 mL ECL cell, and the decrease in ECL intensity was recorded and compared with a standard calibration curve. The Cu^{2+} content in the water sample was determined to be 36.8 ± 0.6 μM (n = 5) which is consistent with the value (37.5 μM) obtained from an inductively coupled plasma-atomic emission spectroscopic method. These results indicate that the analytical performance of our proposed ECL sensor is good and can be applied to determine Cu^{2+} in real samples.

■ CONCLUSIONS

In summary, this paper reports for the first time the ECL responses of the semiconductor g-C$_3$N$_4$, demonstrating that it could be a new class of efficient and promising luminophore for ECL sensing. The possible reaction mechanisms for the ECL are proposed. Since the ECL signals could be effectively quenched by Cu^{2+}, a new approach for sensitive and selective detection of Cu^{2+} has been successfully developed. This study offers an alternative, simple, and cost-effective technique for trace metal ion analysis.

■ ASSOCIATED CONTENT

Ⓢ Supporting Information

Supplementary figures of the XRD pattern, CV curves, chronoamperometry and ECL-time curves in the measurement of relative ECL efficiency, and comparison of the quenching effect of various metal ions on the g-C$_3$N$_4$-based ECL sensor. This material is available free of charge via the Internet at http://pubs.acs.org.

■ AUTHOR INFORMATION

Corresponding Author

*E-mail: xiaodan@scu.edu.cn (D.X.); mfchoi@hkbu.edu.hk (M.M.F.C.).

Notes

The authors declare no competing financial interest.

■ REFERENCES

(1) Wang, X. C.; Maeda, K.; Thomas, A.; Takanabe, K.; Xin, G.; Carlsson, J. M.; Domen, K.; Antonietti, M. *Nat. Mater.* **2009**, *8*, 76−80.

(2) Wang, Y.; Zhang, J. S.; Wang, X. C.; Antonietti, M.; Li, H. R. *Angew. Chem., Int. Ed.* **2010**, *49*, 3356−3359.

(3) Su, F. Z.; Mathew, S. C.; Lipner, G.; Fu, X. Z.; Antonietti, M.; Blechert, S.; Wang, X. C. *J. Am. Chem. Soc.* **2010**, *132*, 16299−16301.

(4) Ding, Z. X.; Chen, X. F.; Antonietti, M.; Wang, X. C. *ChemSusChem* **2011**, *4*, 274−281.

(5) Sun, Y. Q.; Li, C.; Xu, Y. X.; Bai, H.; Yao, Z. Y.; Shi, G. Q. *Chem. Commun.* **2010**, *46*, 4740−4742.

(6) Yan, S. C.; Li, Z. S.; Zou, Z. G. *Langmuir* **2009**, *25*, 10397−10401.

(7) Yan, S. C.; Li, Z. S.; Zou, Z. G. *Langmuir* **2010**, *26*, 3894−3901.

(8) Wang, Y.; Yao, J.; Li, H. R.; Su, D. S.; Antonietti, M. *J. Am. Chem. Soc.* **2011**, *133*, 2362−2365.

(9) Goettmann, F.; Fischer, A.; Antonietti, M.; Thomas, A. *Angew. Chem., Int. Ed.* **2006**, *45*, 4467−4471.

(10) Zhang, Y. J.; Antonietti, M. *Chem. Asian J.* **2010**, *5*, 1307−1311.

(11) Zhang, Y. J.; Mori, T.; Ye, J. H.; Antonietti, M. *J. Am. Chem. Soc.* **2010**, *132*, 6294−6295.

(12) Lee, E. Z.; Jun, Y. S.; Hong, W. H.; Thomas, A.; Jin, M. M. *Angew. Chem., Int. Ed.* **2010**, *49*, 9706−9710.

(13) Li, X. F.; Zhang, J.; Shen, L. H.; Ma, Y. M.; Lei, W. W.; Cui, Q. L.; Zou, G. T. *Appl. Phys. A: Mater. Sci. Process.* **2009**, *94*, 387−392.

(14) Ding, Z. F.; Quinn, B. M.; Haram, S. K.; Pell, L. E.; Korgel, B. A.; Bard, A. J. *Science* **2002**, *296*, 1293−1297.

(15) Miao, W. J. *Chem. Rev.* **2008**, *108*, 2506−2553.

(16) Liang, G. X.; Li, L. L.; Liu, H. Y.; Zhang, J. R.; Burda, C.; Zhu, J. J. *Chem. Commun.* **2010**, *46*, 2974−2976.

(17) Liu, X.; Zhang, Y. Y.; Lei, J. P.; Xue, Y. D.; Cheng, L. X.; Ju, H. X. *Anal. Chem.* **2010**, *82*, 7351−7356.

(18) Wang, J.; Shan, Y.; Zhao, W. W.; Xu, J. J.; Chen, H. Y. *Anal. Chem.* **2011**, *83*, 4004−4011.

(19) Huang, H. P.; Li, J. J.; Zhu, J. J. *Anal. Methods* **2011**, *3*, 33−42.

(20) Bertoncello, P.; Forster, R. J. *Biosens. Bioelectron.* **2009**, *24*, 3191−3200.

(21) Wang, C. Z.; E, Y. F.; Fan, L. Z.; Wang, Z. H.; Liu, H. B.; Li, Y. L.; Yang, S. H.; Li, Y. L. *Adv. Mater.* **2007**, *19*, 3677−3681.

(22) Mei, Y. L.; Wang, H. S.; Li, Y. F.; Pan, Z. Y.; Jia, W. L. *Electroanalysis* **2010**, *22*, 155−160.

(23) Jie, G. F.; Liu, B.; Miao, J. J.; Zhu, J. J. *Talanta* **2007**, *71*, 1476−1480.

(24) Chen, L. F.; Lu, L. L.; Mo, Y.; Xu, Z. M.; Xie, S. P.; Yuan, H. Y.; Xiao, D.; Choi, M. M. F. *Talanta* **2011**, *85*, 56−62.

(25) Hua, L. J.; Han, H. Y.; Chen, H. B. *Electrochim. Acta* **2009**, *54*, 1389−1394.

(26) Zhang, L. H.; Shang, L.; Dong, S. J. *Electrochem. Commun.* **2008**, *10*, 1452−1454.

(27) Cheng, L. X.; Liu, X.; Lei, J. P.; Ju, H. X. *Anal. Chem.* **2010**, *82*, 3359−3364.

(28) Liu, X.; Jiang, H.; Lei, J. P.; Ju, H. X. *Anal. Chem.* **2007**, *79*, 8055−8060.

(29) Jie, G. F.; Liu, B.; Pan, H. C.; Zhu, J. J.; Chen, H. Y. *Anal. Chem.* **2007**, *79*, 5574−5581.

(30) Zhang, L.; Fang, Y. M.; Wang, R. Y.; You, L. X.; Fu, N. Y.; Chen, G. N.; Sun, J. J. *Chem. Commun.* **2011**, *47*, 3855−3857.

(31) Uauy, R.; Olivares, M.; Gonzalez, M. *Am. J. Clin. Nutr.* **1998**, *67*, 952S−959S.

(32) Yan, H. J.; Huang, Y. *Chem. Commun.* **2011**, *47*, 4168−4170.

(33) Wang, Y.; Lu, J.; Tang, L. H.; Chang, H. X.; Li, J. H. *Anal. Chem.* **2009**, *81*, 9710−9715.

(34) Li, L. L.; Liu, H. Y.; Shen, Y. Y.; Zhang, J. R.; Zhu, J. J. *Anal. Chem.* **2011**, *83*, 661−665.

(35) Richter, M. M. *Chem. Rev.* **2004**, *104*, 3003−3036.

(36) Jie, G. F.; Zhang, J. J.; Wang, D. C.; Cheng, C.; Chen, H. Y.; Zhu, J. J. *Anal. Chem.* **2008**, *80*, 4033−4039.

(37) Shan, Y.; Xu, J. J.; Chen, H. Y. *Chem. Commun.* **2009**, 905−907.

(38) Xu, G. B.; Dong, S. J. *Electroanalysis* **2000**, *12*, 583−587.

(39) Niu, H.; Yuan, R.; Chai, Y. Q.; Miao, L.; Yuan, Y. L.; Zhuo, Y.; Yuan, S. R.; Yang, X. *Biosens. Bioelectron.* **2011**, *26*, 3175−3180.

(40) Bae, Y.; Lee, D. C.; Rhogojina, E. V.; Jurbergs, D. C.; Korgel, B. A.; Bard, A. J. *Nanotechnology* **2006**, *17*, 3791−3797.

(41) Yao, W.; Wang, L.; Wang, H. Y.; Zhang, X. L. *Electrochim. Acta* **2008**, *54*, 733−737.

(42) Fabrizio, E. F.; Prieto, I.; Bard, A. J. *J. Am. Chem. Soc.* **2000**, *122*, 4996−4997.

(43) Chen, Y.; Mao, J. F.; Liu, C. H.; Yuan, H. Y.; Xiao, D.; Choi, M. M. F. *Langmuir* **2009**, *25*, 1253−1258.

(44) Chen, Z. F.; Wong, K. M. C.; Kwok, E. C. H.; Zhu, N. Y.; Zu, Y. B.; Yam, V. W. W. *Inorg. Chem.* **2011**, *50*, 2125−2132.

(45) Jang, K. S.; Ko, H. C.; Moon, B. J.; Lee., H. *Synth. Met.* **2005**, *150*, 127−131.

(46) Dai, H.; Chi, Y. W.; Wu, X. P.; Wang, Y. M.; Wei, M. D.; Chen, G. N. *Biosens. Bioelectron.* **2010**, *25*, 1414−1419.

(47) Zou, G. Z.; Ju, H. X. *Anal. Chem.* **2004**, *76*, 6871−6876.

(48) Isarov, A. V.; Chrysochoos, J. *Langmuir* **1997**, *13*, 3142−3149.

(49) Wu, C. L.; Zhao, Y. B. *Anal. Bioanal. Chem.* **2007**, *388*, 717−722.